Mir et al., J Theor Comput Sci 2016, 3:2
DOI: 10.4172/2376-130X.1000147

Journal of
Theoretical & Computational Science

Research Article Open Access

Synthesis and Conjoint Experimental - DFT Characterization of some Pyrazolone Functionalized Dioxovanadium(V) Schiff Base Complexes

Mohammad Mir J, Maurya RC*, Vishwakarma PK, Rajak DK, Jain N, Jaget PS, Parte M, Chaurasia R, Khan MW and Bohre P

Coordination, Bioinorganic and Computational Chemistry Laboratory, Department of PG Studies and Research in Chemistry and Pharmacy, RD University, Jabalpur, Madhya Pradesh, India

Abstract

This paper is concerned with the synthesis and hyphenated DFT-experimental characterization of dioxovanadium(V) complexes of semicarbazones ONO-donor ligands, LH [where, LH=N-(4'-benzoylidene-3'-methyl-1'-phenyl-2'-pyrazolin-5'-one)-semicarbazone (bmphp-semH), N-(4'-butylidene-3'-methyl-1'-phenyl-2'-pyrazolin-5'-one)-semicarbazone (bumphp-semH), N-(4'-*iso*-butylidene-3'-methyl-1'-phenyl-2'-pyrazolin-5'-one)-semicarbazone (*iso*-bumphp-semH) or N-(3'-methyl-1'-phenyl-4'-propionylidene-2'-pyrazolin-5'-one)-semicarbazone (mphpp-semH)] and were prepared from ethanol-methanol mixed solvent (1/10) solutions of bis(acetylacetonato) oxovanadium(IV) complexes of the above ligands by oxidizing with atmospheric oxygen (bubbling air) for 2-3 days. The composition and formulae of complexes were confirmed by various physiochemical analysis, *viz.,* percentage of different elements, magnetic susceptibility, conductance, FT-IR, UV-Visible and mass spectrometry. One of the representative complexes, *cis*-[VO_2(bmphp-sem)(H_2O)] was investigated at the convergence of DFT and experimental formulation interface. The standard B3LYP/LANL2DZ combinations were used to arrive at the approx of geometry optimization, charge distribution and molecular orbital descriptions. The global reactivity parameters like absolute electronegativity (χ_{abs}) and absolute hardness (η) have also been involved. From the overall studies it has been found that the compounds possess *cis*-octahedral structure.

Keywords: DFT; Experimental, dioxovanadium (V); Acylpyrazolone; Electrostatics

Introduction

Acylpyrazolone are attention-grabbing class of pyrazole scaffolds fused to a chelating arm [1] and their synthetic strategies have been evaluated since 1959 [2]. Pyrazolone derivative have been extensively investigated on account of their wide range of pharmacological activities [3]. The search for pyrazolones with excellent therapeutic action [4] and their incorporation into the pharmacopoeia as an antipyretic and, later on, as an analgesic and anti-inflammatory agent is quite fascinating. Nevertheless, the time to time human trials [5] and accompanied toxicity hindrances, added eager to their research scenario and search for less toxic new anti-inflammatory drugs [6] or the preparation of new compounds with antifungal [7], antitumor [8] and antihyperglycemic [9] activities remained an active goal. Very recently, the application of such compounds in apoptosis of Hela cancer cells [10] has been reported. Their metal complexes have shown peculiar redox behavior [11]. The structural determinations of such complexes have gained much attention at both experimental as well as theoretical approaches [12,13].

Semicarbazones on the other hand are also molecules of great interest due to their potential pharmacological properties [14-17]. A variety of semicarbazones and their metal complexes have been reported to possess properties of wide variation in their stereochemistry and modes of bonding through oxygen and azomethine nitrogen atoms [14]. The metal binding properties in semicarbazones are tailored and appended by tagging with different additional donor atoms involving substituted aldehydes or ketones [18-21] witnessed by a number of reports of the same field of investigation [22-24]. Vanadium(V)complexes have been shown to ensue stereo-chemically flexible coordination geometries [25]. The redox behaviour, including V(V)/V(IV) or V(IV)/V(III), increases the versatility of this element in the biological milieu [26]. Unraveling the role of vanadium in normal mammalian metabolism [27] and enlightening its potential therapeutic application have attained mammoth interests [28-30].

Density-functional theory (DFT) is a powerful method for predicting the geometry of vanadium compounds [31-36] including large molecules [37]. The application of theoretical force constants to attain Cartesian representation is useful for the assumption of molecular symmetry. Generally molecular charge topography and orbital analysis provide ample information regarding various reaction parameters [38].

Vanadium in the oxidation state V has been found more potent cell inhibitor and hence, such flexibility of this metal represents the importance in regulatory effects of osteoblasts and is a proof to devise more efficient catalysts. To extend seek for more such types of efficacious compounds of vanadium with neutral charge [28], a systematic study of synthesis and combined DFT-experimental characterization of VO_2^+ complexes of acylsemicarbazones is hereby reported.

Experimental

Materials and methods

3-Methyl-1-phenyl-2-pyrazolin-5-one (Lancaster, UK), benzoyl chloride and propionyl chloride (Thomas Baker Chemicals Ltd., Mumbai), butyryl chloride (S. D. Fine, Chemicals, Baroda), *iso*-butyryl chloride (E. Merck, Germany) and semicarbazide hydrochloride (Sisco Chem. Industries, Mumbai), vanadium pentaoxide [E. Merck (India)

***Corresponding author:** Maurya RC, Coordination, Bioinorganic and Computational Chemistry Laboratory, Department of PG Studies and Research in Chemistry and Pharmacy, RD University, Jabalpur-482 001, Madhya Pradesh, India, Tel: 9753074334; E-mail: rcmaurya1@gmail.com

Received May 06, 2016; **Accepted** June 13, 2016; **Published** June 20, 2016

Citation: Mir MJ, Maurya RC, Vishwakarma PK, Rajak DK, Parte MK, et al. (2016) Synthesis and Conjoint Experimental - DFT Characterization of some Pyrazolone Functionalized Dioxovanadium (V) Schiff Base Complexes. J Theor Comput Sci 3: 147. doi:10.4172/2376-130X.1000147

Ltd., Mumbai], sodium acetate (Fluka AG Co., Switzerland) were used as received. All chemicals used were of analytical reagent (A. R.) grade.

Preparation of different 4-acyl-3-methyl-1-phenyl-2-pyrazolin-5-one (amphp) derivatives

The amphp derivatives were prepared by a slight modification of Jensen's method [39]. Into a one liter 3-necked quick fit flask containing DMF (100 mL) and carrying a dropping funnel, a mechanical stirrer and a reflux condenser was placed 3-methyl-1-phenyl-2-pyrazolin-5-one (0.098 M, 17 g). A solution was obtained by gentle heating and stirring. Calcium hydroxide (0.140 M, 10 g) was added and benzoyl chloride (12 mL)/butyryl chloride (10.33 mL)/*iso*-butyryl chloride (11 mL)/propionyl chloride (8.98 mL) was added drop wise within 3-5 min. The reaction was exothermic and the reaction mixture became a paste. The mixture was allowed to cool and then refluxed with stirring for 1 h on a sand bath during which period the bright yellow complex formed initially turn yellowish brown. The decomposition of complex was carried out by pouring the reaction mixture into a 3N half liter chilled dilute hydrochloric acid solution. As a result yellowish brown solid was obtained that was filtered using sintered glass crucible. Distilled water was used as washing agent and washing was continued until colourless washings were obtained. The final product was dried in air and recrystallized from n-heptane.

Preparation of semicarbazones

Ethanolic solution of semicarbazide hydrochloride (0.05 M, 7.35 g) was first neutralized with sodium acetate solution (0.05 M, 13.9 g). Into this 25 ml of ethanolic solution of bmphpH (0.05 M, 12.20 g), bumphpH (0.05 M, 12.20 g), *iso*-bumphpH (0.05 M, 12.20 g) or mphppH (0.05 M, 11.5 g) was added and was allowed to reflux for 3 h at 60°C with constant stirring. A greenish yellow coloured precipitate was formed that was followed by filtration and washing several times with ethanol. The product was dried in a desiccator over anhydrous calcium chloride (Scheme 1).

Preparation of dioxovanadium (V) complexes

The parent compound, bis(acetylacetonato)oxovanadium(IV), $[VO(acac)_2]$, was prepared by the method of Patel [40]. A hot methanolic solution (25 mL) of $[VO(acac)_2]$ (0.001 M, 0.265 g) was added to the methanolic solution of 25 mL of the respective Schiff base, bmphp-semH (0.001 M, 0.335 g), bumphp-semH (0.001 M, 0.301 g), *iso*-bumphp-semH (0.001 M, 0.301 g) or mphpp-semH (0.001 M, 0.287 g) and was refluxed for 4 h. It was cooled and filtered. The filtrate was collected and the precipitate was dissolved in ethanol-methanol (1:10) and again filtered. The filtrate thus obtained is again added to the above filtrate, which is then kept for air oxidation at room temperature for 3-4 days, with occasional shaking the resulting compound is collected and recrystallized from methanol.

Elemental analysis

Carbon, Hydrogen, and Nitrogen were determined micro-analytically at CDRI, Lucknow. The percentage of vanadium in each of the complexes was determined volumetrically [41] using 0.02 M $KMnO_4$ solution as an oxidizing agent in the presence of sulfurous acid.

Physical methods

Solid-state infrared spectra were reordered in KBr obtained using Perkin-Elmer model 1620 FT-IR spectrophotometer. ^{1}HNMR spectra in DMSO-d_6, elemental analyses (micro-analytically) and mass spectra were recorded at Sophisticated Analytical Instrumentation Facility (SAIF), CDRI, Lucknow. Thermo gravimetric analysis of the complexes was performed on a Perkin-Elmer Thermo analyzer at SAIF, IIT, Bombay. Electronic Spectra were recorded using UV-VIS-Near IR Spectrophotometer (Carry-5000), Agilent Technology, Germany. Magnetic measurements were performed by Gouy`s method using mercury (II) tetrathiocyanatocobaltate (II) as calibrant.

DFT calculation

All the calculations presented in this paper were performed by DFT methods using Gaussian 09 program package [42]. The hybrid exchange-correlation Becke3–Lee–Yang–Parr (B3LYP) functional and LANL2DZ basis sets were used [43,44]. Gauss View 5.0 package was used to have visual display of different harmonic oscillations and to obtain various graphic views of molecular charges and shapes of distinctive molecular orbitals. All the parameters were entertained from the optimized structure (gaseous phase) of the representative compound conditioned to the absence of negative frequency.

Results and Discussion

Synthesis and characterization

Synthesis: The dioxovanadium (V) complexes were prepared according to Scheme 2.

Where LH=bmphp-semH, bumphp-semH, *iso*-bumphp-semH or mphpp-semH.

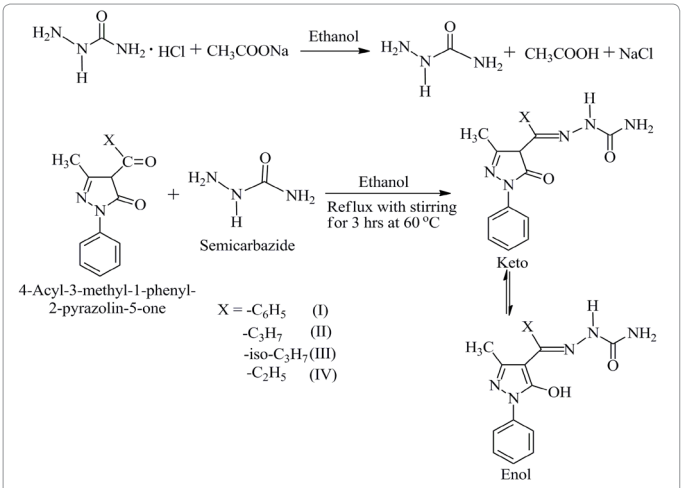

Scheme 1

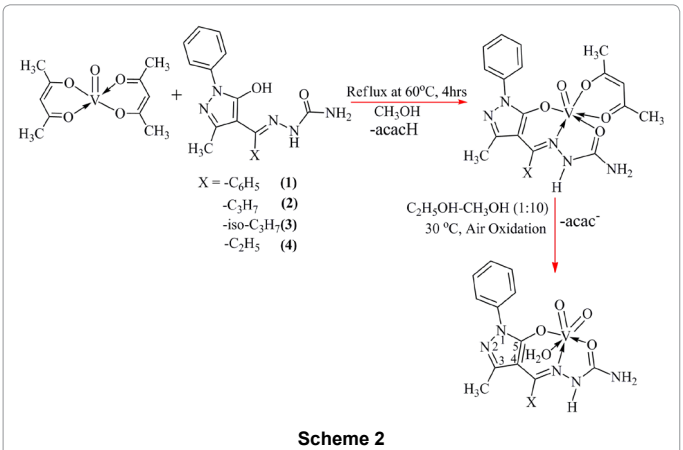

Scheme 2

The synthesized air stable complexes were found thermally stable and the respective decomposition temperatures along with some physical parameters are given in Table 1. From their solubility test it was found that the complexes are insoluble in most of the organic solvents and have shown maximum solubility in DMF. The formulation of these complexes are based on their elemental analysis, FT-IR, ^{1}H-NMR, mass and electronic spectral studies, Thermo gravimetric, magnetic and conductance determinations.

Infrared spectral studies: The important infrared spectral bands of the acylsemicabazone ligands and complexes along with their tentative assignment are given in Table 2. The acylsemicarbazones used in the present investigation may exist in three keto-enol forms (Figure 1). The combined experimental and theoretical IR spectra of a representative complex are given in Figures 2 and 3. All the four acylsemicarbazones exhibit a weak band centered at 3360-3410 cm^{-1} for ν(OH), a strong band at 1681-1695 cm^{-1} for ν(C=O) (semicarbazide skeleton) and another strong band due to ν(C=N) (azomethine) at 1612-1650 cm^{-1}. The presence of NH vibrational mode of hydrazide at 3125-3138 cm^{-1} and stretching frequency of -NH_2 at 3340-3380 cm^{-1} and 3214-3238 cm^{-1} was observed in the infrared spectra of all the acylsemicabazones. Hence culminates that the semicarbazone ligands under the question exist in enol form [**II**] in the solid state. Recently for such chemical moieties the hyderogen bonding between C=O oxygen and adjacent NH- hydrogen stems the same assumption [45].

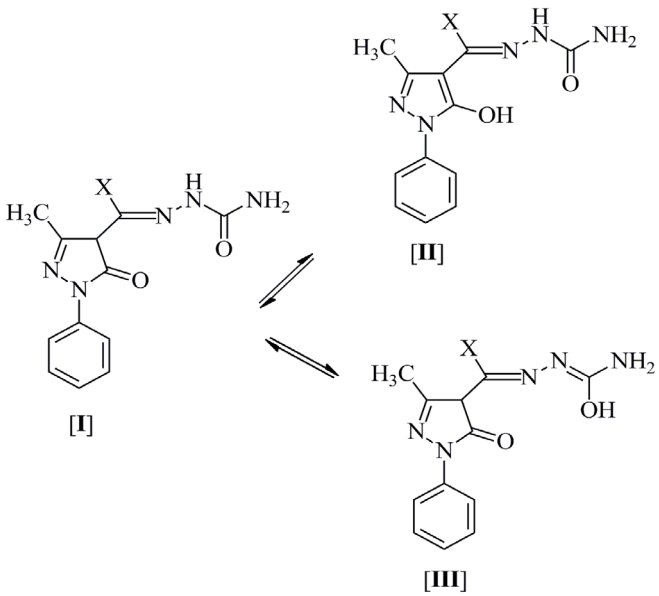

Figure 1: Keto-*enol* forms of synthesized Schiff Bases.

Compounds Empirical formula (M.W.)	Found (calcd.), (%)				Color	Decomp. Temp. (°C)	Λ_M ($\Omega^{-1}cm^2mole^{-1}$)	Yield (%)
	C	H	N	V				
bmphp-semH $C_{18}H_{17}N_5O_2$ (335)	64.56 (64.47)	5.12 (5.07)	20.76 (20.89)	-	Yellow	200	-	72
bumphp-semH $C_{15}H_{19}N_5O_2$ (301)	59.36 (59.80)	6.25 (6.31)	23.45 (23.25)	-	Yellow	160	-	66
iso-bumphp-semH $C_{15}H_{19}N_5O_2$ (301)	59.75 (59.80)	6.53 (6.31)	23.43 (23.25)	-	Yellow	163	-	69
mphpp-semH $C_{14}H_{17}N_5O_2$ (287)	58.64 (58.53)	5.84 (5.92)	24.53 (24.39)	-	Yellow	169	-	62
$[VO_2$(bmphp-sem)$H_2O]$(**1**) $C_{18}H_{18}N_5O_5V$ (435.76)	49.60 (49.32)	4.16 (4.35)	16.07 (16.25)	11.68 (11.35)	Pepper-ment	258	12.6	60
$[VO_2$(bumphp-sem)$H_2O]$(**2**) $C_{15}H_{20}N_5O_5V$ (401.3)	44.89 (44.36)	5.02 (5.28)	17.46 (17.58)	12.69 (12.85)	Lime	250	14.5	72
$[VO_2$(iso-bumphp-sem)$H_2O]$ (**3**) $C_{15}H_{20}N_5O_5V$ (401.3)	44.89 (44.56)	5.02 (5.65)	17.46 (17.32)	12.69 (12.52)	Light olive	235	16.3	68
$[VO_2$(mphpp-sem)$H_2O]$(**4**) $C_{14}H_{18}N_5O_5V$ (387.27)	43.42 (43.25)	4.68 (4.25)	18.09 (18.36)	13.15 (13.52)	Cascade Green	263	14.6	65

Table 1: Analytical data and some physical properties of the synthesized Schiff-bases and its complexes.

Compounds	$\nu_s(VO_2)$	$\nu_{as}(VO_2)$	ν(C=O) Semi	ν(C=N) Azomethine	ν(C=N) Pyrazolinring	ν(C-O) Enolic	ν(NH)	ν(NH_2)	ν(OH)
(bmphp-semH)	-	-	1695	1650	Merged with ν(C=N) azo	1210	3138	3348 3216	3360
(bumphp-semH)	-	-	1694	1612	Merged with ν(C=O)	1250	3130	3340 3214	3390
(*iso*-bumphp-semH)	-	-	1695	1615	Merged with ν(C=N) azo	1210	3138	3380 3230	3410
(mphpp-semH)	-	-	1681	1620	Merged with ν(C=N) azo	1256	3125	3350 3238	3380
$[VO_2$(bmphp-sem)$H_2O]$(**1**)	860	952	1659	1595	Merged with ν(C=N) azo	1261	3148	Merged with ν(OH)	3420
$[VO_2$(bumphp-sem)$H_2O]$(**2**)	814	909	1609	Merged with ν(C=O)	Merged with ν(C=O)	1270	3140	Merged with ν(OH)	3440
$[VO_2$(iso-bumphp-sem)$H_2O]$(**3**)	817	908	1615	1593	Merged with ν(C=N) azo	1280	3130	Merged with ν(OH)	3380
$[VO_2$(mphpp-sem)$H_2O]$(**4**)	839	979	1634	1590	Merged with ν(C=N) azo	1278	3110	Merged with ν(OH)	3471

Table 2: IR spectral data of the synthesized Schiff-bases and their complexes.

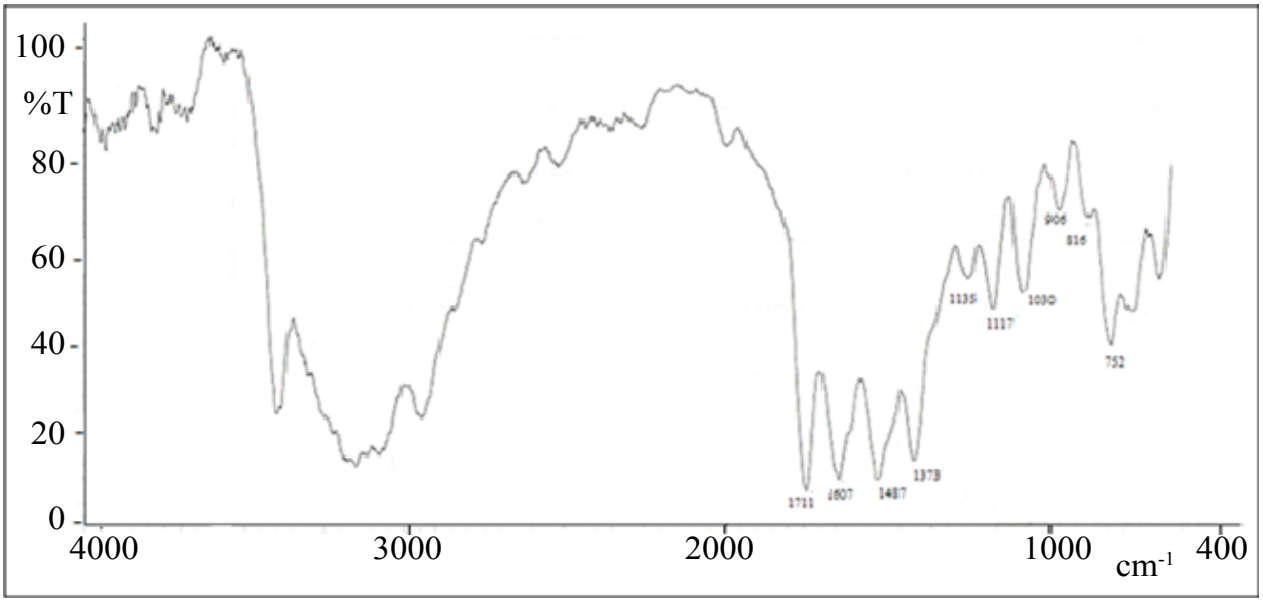

Figure 2: FT-IR spectrum of (bmphp-semH) Schiff base.

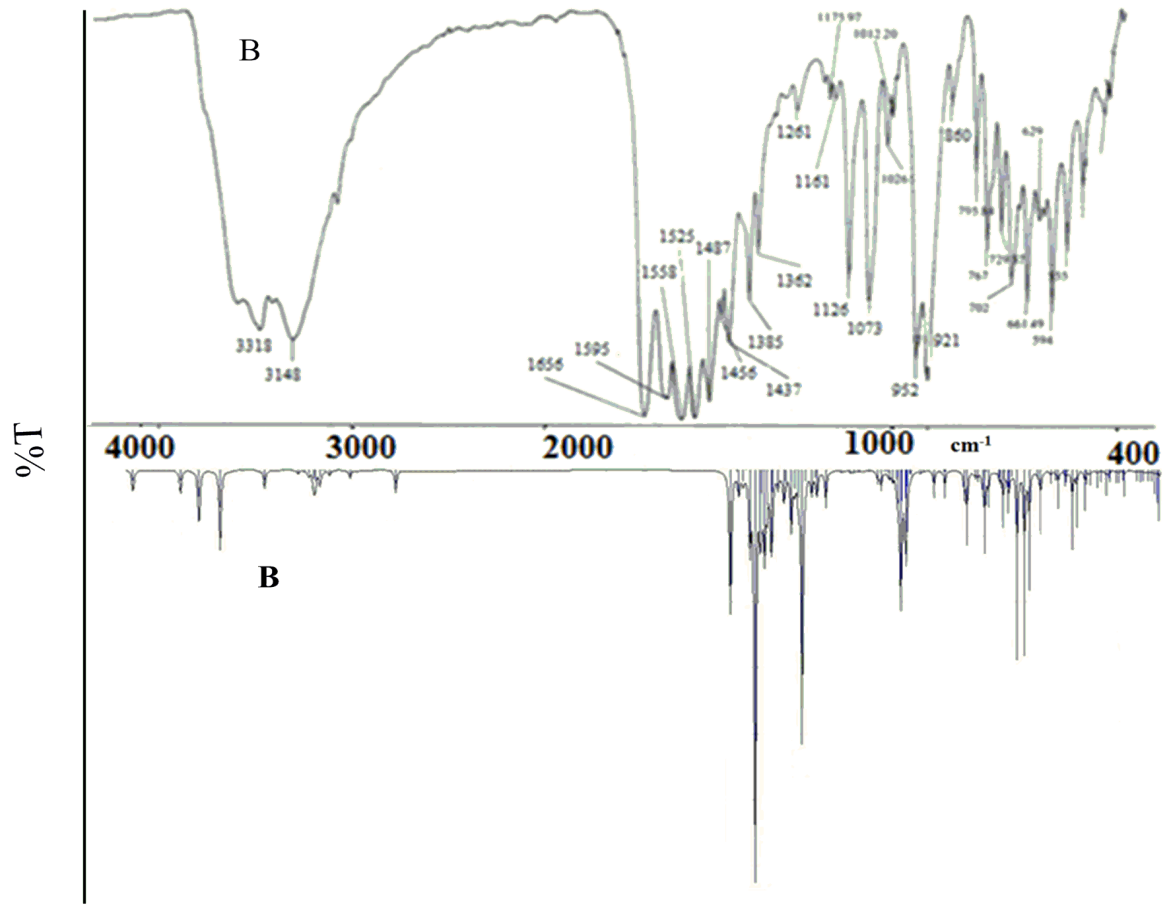

Figure 3: Experimental (A) and theoretical (B) IR spectra of [VO_2(bmphp-sem)(H_2O)], (1).

In the light of enol form [**II**], these four semicarbazone ligands possess seven potential donor sites: (i) the ring nitrogen N^1 (ii) the ring nitrogen N^2 (iii) the cyclic enolic oxygen (OH), (iv) azomethine nitrogen, (v) the hydrazide nitrogen, (vi) amide oxygen and (vii) amide nitrogen. The coordination of ring nitrogen N^1 is unlikely due to presence of bulky phenyl group on it [46]. The appearance of $\nu(C=N^2)$ (cyclic) mode 1593 cm^{-1} at almost the same position {here merged with $\nu(C=N)$ (azomethine)} compared to $\nu(C=N^2)$ (cyclic) at ~1590 cm^{-1} of the uncoordinated ligand, after complexation gestures that the ring nitrogen N^2 in these ligands is found to be inert towards coordination to vanadium. The coordination binding of enolic oxygen after deprotonation hints the disappearance of ν(OH) at 3360-3410 cm^{-1} in the spectra of the complexes. But due to ν(OH) of coordinated water (*vide infra*), it creates ambiguity to clarify the coordination of enolic oxygen. However, metal-enolic oxygen bond is confirmed by ν(C-O) (enolic) [47] at 1261-1280 cm^{-1} compared to ν(C-O) (*enolic*) at 1210-1256 cm^{-1} in the uncoordinated ligands.

The ν(CO) mode of amide carbonyl group observed at 1681-1695 cm^{-1} in the ligands is shifted to lower wave numbers [48] and appears at 1609-1659 cm^{-1} in these complexes. This suggests the bonding of the amide carbonyl oxygen to vanadium in all these complexes. The acylsemicabazones in the present discussion display a sharp and strong band due to ν(C=N) of the azomethine group at 1612-1650 cm^{-1}. The observed low energy shift [49] of the band in the complexes at 1590-1595 cm^{-1} suggests the coordination of the azomethine nitrogen to vanadium. The vanadium binding with azomethine nitrogen, cyclic enolic oxygen and amide carbonyl oxygen as discussed above favours the formation of the complexes having six and five membered rings in coordination sphere [50]. In view of this, the coordination of hydrazide nitrogen and amide amino nitrogen is ruled out. This is further supported by the no appreciable change in the ν(NH) (hydrazide nitrogen) and $\nu(NH_2)$ (amide amino group) of the ligands after complexation. The overall infrared spectral studies conclude that the acylsemicarbazones used in the present study behave as monobasic tridentate ONO-donor ligands.

All the metal chelates also show medium/broad band at 3327-3471 cm^{-1} due to ν(OH) mode because of the presence of lattice/ coordinated water in them. Besides, two sharp bands at 908-979, and 814-860 cm^{-1} (experimental), 1045 and 1027 cm^{-1} (theoretical) correspond to ν_{as}(O=V=O) and ν_s(O=V=O) modes, respectively of the *cis*-VO_2 moiety [51-53] are also discussable. Figure 3 indicates the similarities between theoretical and experimental FT-IR results and hence ascertains the true value of proposed functional group vibrations. Hence, the involved level of theory of computation is quite reliable. The FTIR spectra of two representative Schiff bases are given in Figures 2 and S1. While, Figures S2-S4 are infrared spectra of the synthesized complexes.

Electronic spectral studies: The electronic spectroscopic insights of two representative compounds were gained from their 10^{-3} M DMF solution and the results are given in Table 3. These two complexes displayed two intra-ligand transitions in the ultraviolet region. The 3rd spectral peak at ~378 nm in the complexes is due to ligands → metal charge transfer (LMCT) transition. These results are comparable to the data reported elsewhere [54,55] for dioxovanadium(V) complexes. The theoretical electronic spectrum of representative complex was calculated using the TD-DFT method with the PCM solvent model, using DCM as the solvent. The core information regarding oscillatory strengths, transition energies and excitation coefficients were obtained for complex (1). Transitions bearing largest oscillator strengths are retained, however for a long wave part the transitions with small oscillator strengths are also given in Figures 4a and 4b and the respective theoretical electronic spectrum data have been shown in Table 4.

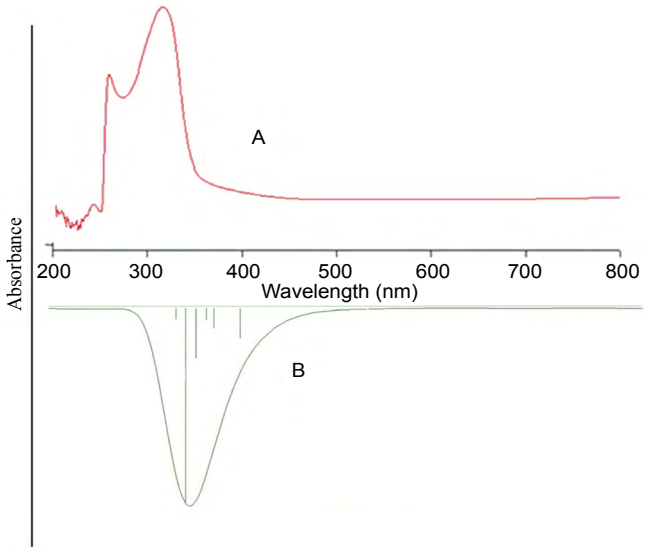

Figure 4: Experimental (A) and TD-DFT based (B) electronic spectrum of *cis*-[VO_2(bmphp-sem)(H_2O)], (1).

Complexes	λ_{max} (nm)	ν (cm^{-1})	Peak Assignment
[VO_2(bmphp-sem)(H_2O)]	245	40816	Intra ligand Transitions
	260	38441	Intra ligand Transitions
	378	26455	Ligand to Metal Charge Transfer Transitions (L→ M)

Table 3: Electronic spectral data of the synthesized complexes.

ΔE (eV)	λ/nm Calc.	*f*	λ/nm Exp.	Assignments
3.0308	409.07	0.0219	401	Ligand to Metal Charge Transfer Transitions (L→ M)
3.2811	377.87	0.0146	-	π- π* intra ligand charge transfer
3.3615	368.84	0.0083	-	π- π* intra ligand charge transfer
3.4786	356.42	0.0368	-	π- π* intra ligand charge transfer
3.6004	344.36	0.1427	347	π- π* intra ligand charge transfer
3.7256	332.79	0.0079	300	π- π* intra ligand charge transfer

Table 4: Theoretical electronic spectrum of the complex [VO_2(bmphp-sem)(H_2O)], (1) calculated with the TD-DFT method in DMSO solvent.

Conductance measurements: From molar conductance determination the respective assignments of the synthesized complexes in 10^{-3} M DMF solution have been found in the range of 12.6-16.3 $ohm^{-1}cm^2mol^{-1}$ (Table 1). From the results the non-electrolytic nature of these complexes is inferred. The strong donor capacity of DMF, the displacement of anionic ligand and change of electrolyte type are supposed the reasons that develop the non-zero reading [56].

Magnetic measurements: As expected for dioxovanadium (V) compounds [40], the observed magnetic moments (0.23-0.78 BM) show diamagnetic behaviour of this class of complexes.

Mass spectrometry insights: The fast atomic bombardment (FAB) type of mass spectrometry carried out for a representative complex *cis*-[VO_2(mphpp-sem)(H_2O)] (4), Figure 5 was recorded on a JEOL SX 12/DA-6000 Mass Spectrometer/Data system using Xenon/Argon (6 KV, 10 mA) as the FAB gas in the m/z range 86.35-1111.42. The mass spectral peaks observed at 136, 137, 154, 289 and 307 m/z are

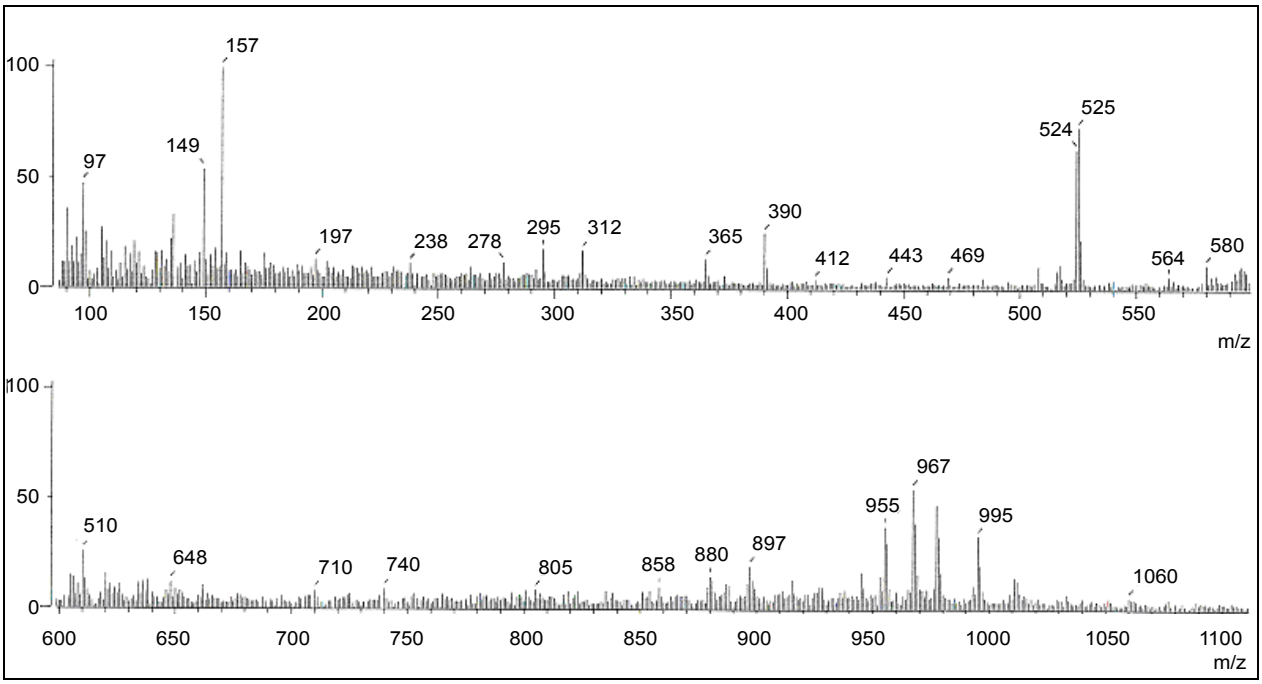

Figure 5: Mass spectrum of *cis*-[VO_2(mphpp-sem)(H_2O)] (1).

matrix [*m*-nitrobenzyl alcohol (NBA)] peaks. The appearance of a peak at 365 m/z is consistent with molecular mass of the present compound excluding one water molecule present therein, which is supposed to be lost before ionization. The other mass spectral signals observed at, 365, 441, 524 and 525 m/z in the complex might be because of the following types of ion aggregations:

$[VO_2(mphpp\text{-}sem)]^+$ (369)-4$[H]^+$=365

$[(mphpp\text{-}sem)]^+$ (285)+$[matrix]^+$ (154)+2$[H]^+$=441

$[VO_2(mphpp\text{-}sem)]^+$ (369)+$[matrix]^+$ (154)+$[H]^+$=524

$[VO_2(mphpp\text{-}sem)]^+$ (369)+$[matrix]^+$ (154)+2$[H]^+$=525

The mass spectral data shows close agreement with the supposed molecular structure of the complex (**4**).

^{1}NMR spectral studies: The proton NMR spectrum of a representative compound, namely, *cis*-[VO_2(bmphp-sem)(H_2O)] (**1**) Figure 6, was recorded in DMSO-d_6 using TMS as a reference. This compound displays a multiplet of proton signal due to aromatic protons of phenyl group at δ 7.22-7.94 ppm and a singlet at δ 10.11 ppm due to –NH proton of hydrazide moiety. The proton signals at δ 3.33 and 1.34 ppm are most probably due to proton groups such C-NH_2 (**b**), -C-CH_3 (**a**), respectively present in this compound. The proton signal at 2.51 ppm is most probably due to solvent (DMSO-d_6) taken. The nonappearance of enolic proton signal at ~ 12 ppm in the complex (deprotonation of -OH) points the coordination of enolic oxygen with the metallic centre. The indexing of various proton groups is given in the Figure 5. The ^{50}V NMR spectrum of the model compound, *cis*-[VO_2(bmphp-sem)(H_2O)] (1), Figure 7 was recorded in DMSO-d_6. The complex exhibits a strong resonance at ca. -508.90, as expected for the dioxovanadium(V) complexes having a mixed O/N donor set.

Thermogravimetric studies: Thermo gravimetric curve of *cis*-[VO_2(bmpph-sem)(H_2O)] (**1**), was recorded in the temperature range of 25-1000°C with the heating rate of 15°C /min (Figure 8). The compound (**1**) shows a weight loss of 4.44% at 170°C (Calcd. weight loss of one mole H_2O, 4.13%) corresponding to the elimination of one molecule of coordinated water [52]. This compound shows further weight losses beyond 300°C and upto 980°C in three steps, which unfortunately could not be correlated separately. However, the final weight loss of 75.6% observed at 980°C corresponds to the elimination of one (bmphp-sem) ligand group and one water molecule (calcd. weight loss, 81%). The final residue (obs.=24.4%) roughly corresponds to V_2O_5 (calcd.=19.0%).

The proposed sequential representation of the thermal decomposition of complex may be shown as below:

$$[C_{18}H_{18}N_5O_5V] \xrightarrow{20-170^\circ C} [C_{18}H_{16}N_5O_4V]$$

$$[C_{18}H_{16}N_5O_4V] \xrightarrow{171-340^\circ C} [C_{17}H_{14}N_3O_3V]$$

$$[C_{17}H_{14}N_3O_3V] \xrightarrow{341-580^\circ C} [C_9H_8NO_3V]$$

$$[C_9H_8NO_3V] \xrightarrow{581-980^\circ C} [V_2O_5]$$

DFT studies

Molecular geometry: The main elements of optimized geometry of the title compound, *cis*- [VO_2(bmphp-sem)(H_2O)] including interatomic distances and the angle of orientation of different bindings are shown in Table S1. The structure appears to have a little distorted octahedral geometry (Figure 9). It is observed that, the length of V=O bond fall in the range of 1.61-1.62 Å for dioxovanadim complex it is very close agreement with experimental values [49]. The computed bond lengths, such as, V-O(2),(oxo) V-O(3),(oxo) V-O(4), (enolic), V-N(5)(azo), V-O(6)(ketonic) and V-O(7) water in the present complex are 1.619, 1.612, 1.888, 2.531, 2.021, and 2.403 Å, respectively. The bond angles in the coordination sphere of the complex, such as, O(3)-V(1)-O(2)(105.117), O(4)-V(1)-O(2)(103.987), O(4)-V(1)-O(3) (105.388), N(5)-V(1)-O(2)(87.204), N(5)-V(1)-(3)(166.601), N(5)-V(1)-O(4)(73.222°), O(6)-V(1)-O(2)(96.288), O(6)-V(1)-O(3)

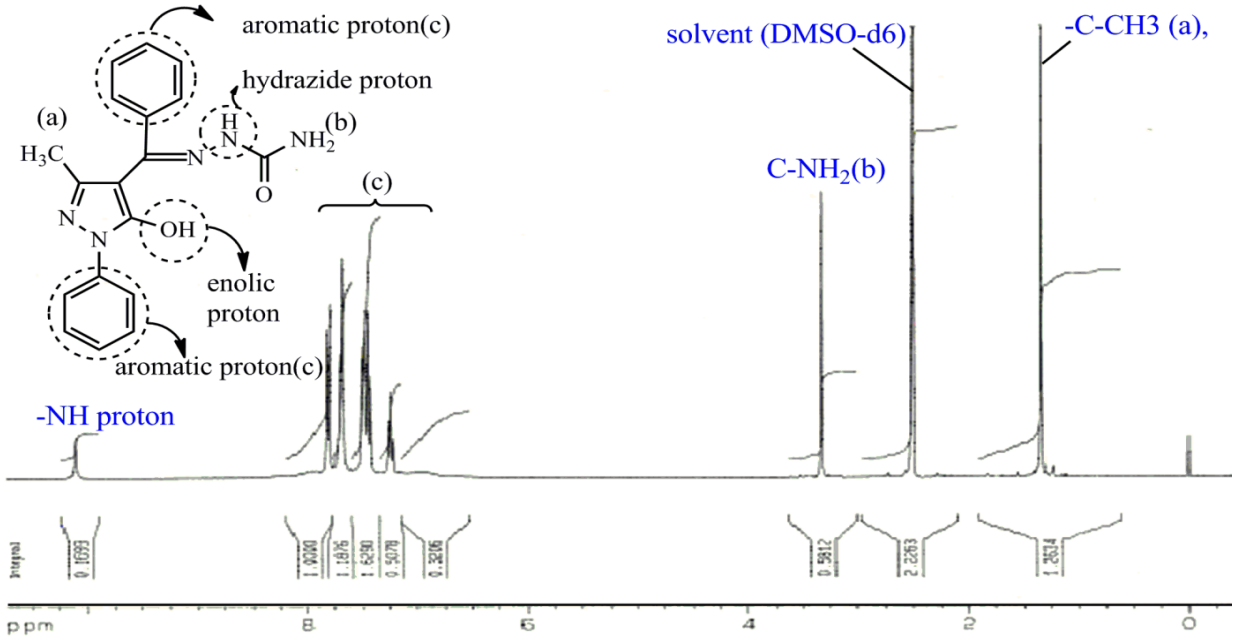

Figure 6: ^{1}HNMR spectrum of *cis*-[VO_2(bmphp-sem)(H_2O)] (1).

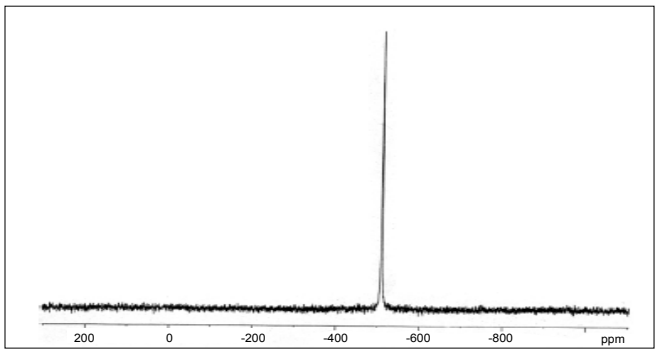

Figure 7: ^{51}VNMR spectrum of *cis*-[VO_2(bmphp-sem)(H_2O)] (1).

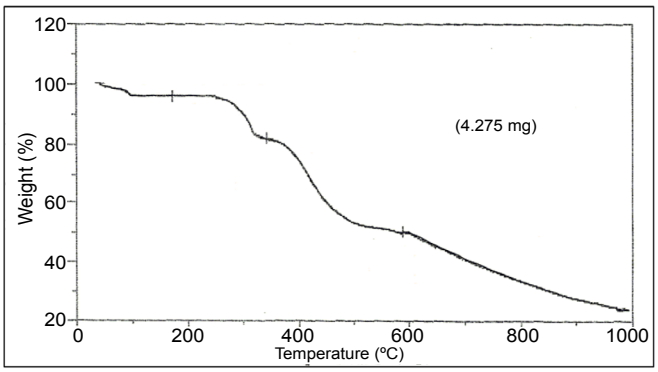

Figure 8: TG curve of *cis*-[VO_2(bmpph-sem)(H_2O)] (1).

(102.729), O(6)-V(1)-O(4)(138.928), O(6)-V(1)-N(5)(72.574), O(7)-V(1)-O(2)(163.250), O(7)-V(1)-O(3) (89.962), O(7)-V(1)-O(4) (76.915), O(7)-V(1)-N(5)(76.915) and O(7)-V(1)-O(6)(73.902) (°) revealed the octahedral geometry of the compounds [56].

Molecular orbital approach: Highest Occupied Molecular Orbitals (HOMO) and Lowest Unoccupied Molecular Orbitals are very significant elements of theoretical molecular design [57]. The intermolecular and intramolecular interaction can be predicted by this way. Hence, the name "Frontier orbitals" emerged. The HOMO is electron donor and LUMO the electron acceptor sites, and the HOMO-LUMO gap speculates the molecular hardness and softness of a compound [58]. Six molecular orbitals (MOs), *viz.*, [HOMO-2], [HOMO-1], [HOMO], [LUMO], [LUMO+1] and [LUMO+2] are worked out for the complex [VO_2(bmphp-sem)(H_2O)]and the respective observed energies are as -6.5271, -6.00547, -5.60982,-1.70760, -1.08327, -0.96327 eV, while the energy difference between [HOMO-LUMO], [HOMO-1-LUMO+1] and [HOMO-2-LUMO+2] are : 3.90222, 4.9222, 5.56383 eV, respectively. The electronic configuration of MO's in shows the presence of paired electron in the HOMO justifying the diamagnetic nature of the investigated complex.

Energy of the frontier orbitals is related to the ionization energy (IE) and electron affinity (EA) derived from Koopmans's theorem [59], and is given as:

$-E_{HOMO}$=IE, …….. (i)

$-E_{LUMO}$=EA, ……. (ii)

While as, IA and EA are related to absolute electronegativity (χ_{abs}) and absolute hardness [60] as given below:

χ_{abs}=(IE + EA)/2=(E_{HOMO}+E_{LUMO})/2 ……(iii)

η=(IE - EA)/2=(E_{HOMO}-E_{LUMO})/2 …….(iv)

Hard molecules have a large HOMO-LUMO gap, and soft molecules have a small HOMO-LUMO gap [61,62]. All the global reactive descriptors were calculated and are represented in Table S2. The molecular orbital structures with energy level description of the complex [VO_2(bmphp-sem)(H_2O)] is displayed in Figure 10.

Other important properties correlated with dipole moment and hardness are electrophilicity index (ω) and global softness (S)

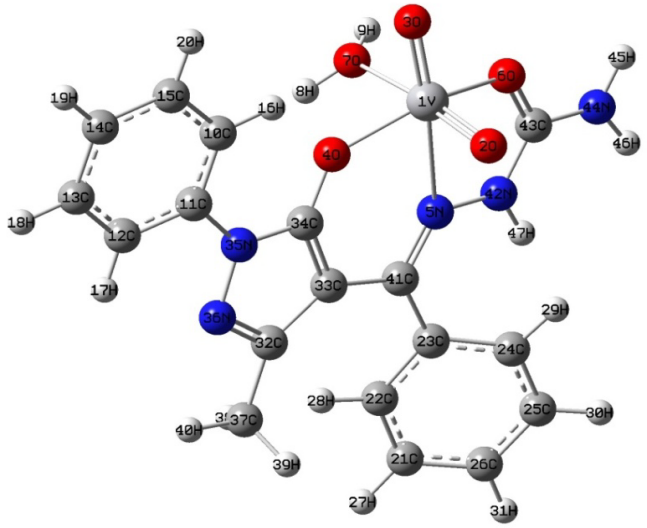

Figure 9: Molecular Structure of *cis*-[VO_2 (bmphp-sem)(H_2O)].

(equations shown below). The numerical assignments of ω and S are tabulated in Table S2.

$\omega=\mu^2/ 2\eta$ .....(v)

$S=1/\eta$ .....(vi)

Atomic net charges: In order to determine delocalization of electron density between occupied Lewis-type orbitals and unoccupied non-Lewis NBOs (antibonding or Rydberg) (Table S3), which eables to find donor–acceptor interaction [63] atomic charges analysis of *cis*-[VO_2(bmphp-sem)(H_2O)] complex was fetched by the computational output data. The largest negative charges are located on the two oxygen atoms, O (7); (-0.93658e) and O (4); (0.62491e). Thus, the bond lengths of V-O (7) and V-O (4) see are different. The electron configuration of V is: [core] 4s(0.01)3d(3.60)4p(0.40)5s(0.22)4d(0.06) according natural bond orbital analysis. Thus, (17.9946) core electrons, (4.21610) valence electrons (on 4s, 3d, and 4p atomic orbitals) and 0.07309 Rydberg electrons (mainly on 5s, and 4d orbitals) give the 22.25980 electrons. This is in good approx with the calculated natural charge on vanadium atom (+0.74020) in the complex, which corresponds to the difference between 22.25980e and isolated V atom's total electron count (23e). In addition, the five oxygen atoms and one nitrogen atoms have larger negative charge as shown in Table S3. Thus, the positive atomic charge upon the vanadium (V) was substantially reduced as a consequence of electron density donation from ligands. According to Table S3 and S4, the calculated electron density on the donor atoms of oxygen and nitrogen atoms is less than expected, while the electron density computed on the central ions is more than expected. These observations lay confirmation of electron transmission between donor atoms and central metal ion.

The natural atomic charges of *cis*-[VO_2(bmphp-sem)(H_2O)] obtained by two main methods of population analysis, Natural population analysis (NPA) and Mulliken population analysis are compared in Table S4. It is not an easy task to compare between Mulliken's net charges and the atomic natural ones because of the difference in their backgrounds. It is further explained by considering the results showing surprisingly well pronounced differences between the two sets of charges. The observation indicates that the atoms namely C_{11}, C_{32}, C_{34}, C_{41}, C_{43}, and all hydrogen's including V are positively charged both in NPA and Mulliken analyses. The remaining atoms: C_{12}-C_{15}, C_{21}, C_{22}, C_{24}-C_{26}, C_{33}, C_{37}, and all oxygen namely O_2, O_3, O_4, O_5, O_6, O_7 and N_5, N_{35}, N_{36}, N_{42}, N_{44} are showing negative partial charges over them in both the analysis. While C_{23} bear positive charge in Mulliken analyses and negatively charge in NPA. The graphical representation of NBO and Mulliken charges of complex is given in Figure 11.

From the literature survey it has been suggested that the natural atomic charge is based on the theory of the natural population analysis. NBOs have been supposed as the linear combinations of the natural atomic orbitals. It may be added here that natural population analysis always follows Pauli's exclusion principle [64].

Molecular electrostatic potential surface (meps) of complex: The molecular surface charge topography is a significant concept to localize the reactive behavior of a molecule with respect to different atomic constituents varying in nature. Under such question negative regions can be assigned as nucleophilic centers, whereas the positive regions are designated as potential electrophilic loci. It is a graphical presentation to display the molecular electrostatic potential pointing to molecular shape, size and electrostatic potential values and also can be related to various biochemical and physical phenomena. Figure 11 clearly presents the nature of various atoms in coordination environment. Five oxygen atoms and one nitrogen atom around vanadium is the region of most negative potential. The hydrogen atoms bear the region

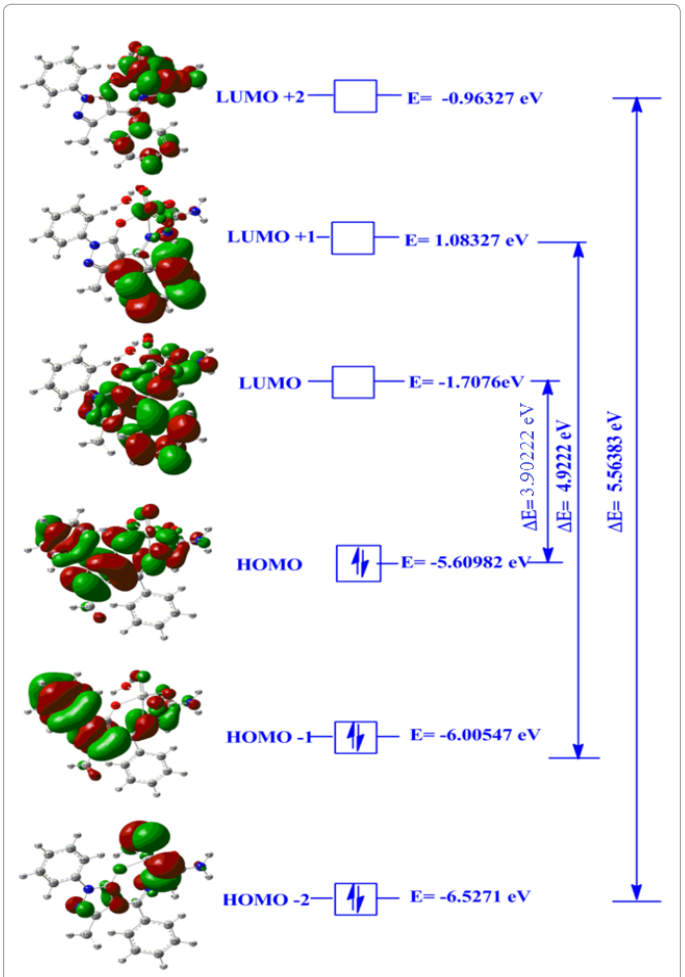

Figure 10: HOMO and LUMO Molecular orbital diagram of *cis*-[VO_2(bmphp-sem)(H_2O)].

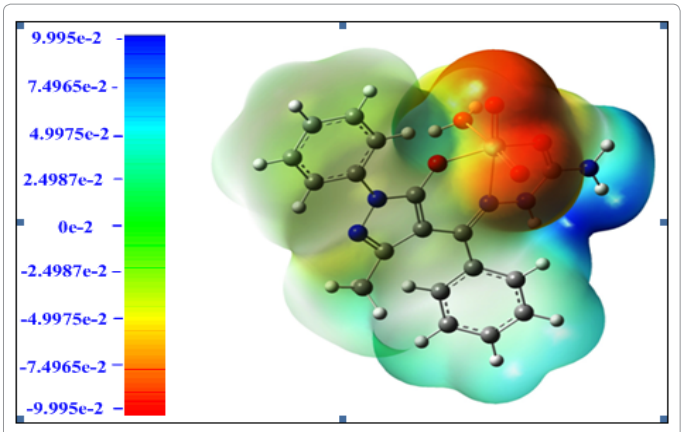

Figure 11: B3LYP/6-31G(d) calculated 3D molecular electrostatic potential of *cis*-[VO_2(bmphp-sem)(H_2O)] complex in atomic units (a.u.) mapped on the electronic density isosurface of 0.02 a.u.

of maximum positive charge, especially the hydrogens of Schiff base ligand. The two hydrogens attached to the electronegative oxygen of the coordinated water molecule are most electropositive constituents. The green region in the MESP surfaces refers to a halfway potential between the two extremes red and dark blue colors. In other words it is the midpoint location between the extreme electronegative and electropositive sites.

Conclusion

From the combined experimental and theoretical approach dioxovanadium(V) complexes synthesized in this investigation are of the general composition [VO_2(L)(H_2O)] where LH=N-(4'-benzoylidene-3'-methyl-1'-phenyl-2'-pyrazolin-5'-one)-semicarbazone (bmphp-semH), N-(butyrylidene -3'-methyl-1'-phenyl-2'-pyrazolin-5'-one)-semicarbazone (bumphp-semH), N-(4'-*iso*-butyrylidene -3'-methyl-1'-phenyl-2'-pyrazolin-5'-one)-semicarbazone (*iso*-bumphp-semH) or 3'-methyl-1'phenyl-4'-propiolidene-2'-pyrazolin-5'-one)-semicarbazone (mphpp-semH)]. Keeping in view the monomeric hexa-coordination of all the complexes, and the well-established octahedral structure of dioxovanadium(V) complexes, K[VO_2(sal-iNH)(H_2O)] and K[VO_2(Clsal-iNH)(H_2O)] involving N-isonicotinamido-salicylaldimines(aroylhydrazones) ligand (similar to LH in the present investigation), *cis*-octahedral structure (Figure 9) has been proposed for this class of complexes. X-ray crystallographic studies, which might confirm the proposed structures, could not be carried out, as suitable crystals were not obtained. The theoretical structural parameters have shown an excellent agreement with the experimental results and hence stem the fact of the reliability of the employed level of theory. In order to endure the investigative boost with respect to such class of compounds it is inferred that the target compounds might prove helpful in framing durable and long lasting materials.

Acknowledgements

The authors are thankful to Vice Chancellor Prof. Kapil Dev Mishra, Rani Durgavati University, Jabalpur, Madhya Pradesh, India for encouragement. Analytical facilities provided by the Central Drug Research Institute, Lucknow, India and the Regional Sophisticated Instrumentation Centre, Indian Institute of Technology, Mumbai, India are gratefully acknowledged. Refer supplementary material for Tables S1-S4 and Figures S1-S4.

References

1. Marchetti F, Pettinari C, Pettinari R (2005) Acylpyrazolone ligands: Synthesis, structures, metal coordination chemistry and applications. Coord Chem Rev 249: 2909-2945.
2. Jensen BS (1959) The Synthesis of 1-Phenyl-3-methyl-4-acyl-pyrazolones-5. Acta Chem Scand 13: 1668-1670.
3. Alaudun M, Sushama PG, Dorothy AM (2003) Studies on synthesis, characterisation, molecular modeling and antimicrobial activity of some metal chelates of pyrazolone based ligands. Indian J Chem 42A: 1617-1621.
4. Goodman G, Rall TW, Nies AS, Taylor P (1996) Goodman and Gilman's. The Pharmacological Basis of Therapeutics. 8th edn. Pergamon Press, Oxford, UK.
5. Wiley HR, Wiley P (1964) Chemistry of Heterocyclic Compounds: Pyrazolones, Pyrazolidones, and Derivatives.
6. Clark MP, Bookland RG (2005) Pyrazolones as therapeutics for kinase-mediated inflammatory disorders. Expert Opin Ther Pat 15: 1617-1623.
7. Omotowa, Mesubi MA (1997) Correlation of Coordination Geometries and Stability Factors in Organotin(IV) Derivatives of 4-Acylpyrazol-5-onates with their Fungicidal (Mycelial Control) and Insecticidal (Topical Toxicity, Larvicidal and Ovicidal) Activities. Appl Organomet Chem 11: 1-10.
8. Caruso F, Rossi M, Tanski J, Sartori R, Sariego R, et al. (2000) Synthesis, structure, and antitumor activity of a novel tetranuclear titanium complex. J Med Chem 43: 3665-3670.
9. Kees KL, Fitzgerald JJ Jr, Steiner KE, Mattes JF, Mihan B, et al. (1996) New potent antihyperglycemic agents in db/db mice: synthesis and structure-activity relationship studies of (4-substituted benzyl) (trifluoromethyl) pyrazoles and -pyrazolones. J Med Chem 39: 3920-3928.
10. Zhao B, Shang X, Xu L, Zhang W, Xiang G (2014) Novel mixed ligand di-n-butyltin (IV) complexes derived from acylpyrazolones and fluorinated benzoic acids: synthesis, characterization, cytotoxicity and the induction of apoptosis in Hela cancer cells. Eur J Med Chem 76: 87-97.
11. Zhang HH, Li JZ, Zhang HQ, Peng L (2014) Synthesis, crystal structure and electrocatalytic behavior of a copper (II) complex derived from acylpyrazolone double Schiff bases. Cryst Res and Tech 49: 171-177.
12. Sharma N, Parihar S, Jadeja RN, Kant R, Gupta VK (2014) Crystal structure of (4Z)-1-(3,4-di-chloro-phen-yl)-4-[hy-droxy(4-methyl-phen-yl)methyl-idene]-3-methyl-4,5-di-hydro-1H-pyrazol-5-one. Acta Crystallogr Sect E Struct Rep 70: 1136-1137.
13. Parihar S, Gupta SK, Jadeja RN, Jha PK(2014) A comparative study of experimental and theoretical results of conformations of oxovanadium (IV) complexes with 4-acyl pyrazolone ligands using DFT method. Spectrochim Acta A Mol Biomol Spectrosc 128: 447-451.
14. Beraldo H, Gambino D (2004) The wide pharmacological versatility of semicarbazones, thiosemicarba-zones and their metal complexes. Mini Rev Med Chem 4: 31-39.
15. West DX, Sonawane PB, Kumbhar AS, Yerande RG (1993) Thiosemicarbazone complexes of copper (II): Structural and biological studies. Coord Chem Rev 123: 49-71.
16. Sridhar SK, Pandeya SN, Stables JP, Ramesh A (2002) Anticonvulsant activity of hydrazones, Schiff and Mannich bases of isatin derivatives. Eur J Pharm Sci 16: 129-132.
17. Yogeeswari P, Ragavendran JV, Sriram D, Nageswari Y, Kavya R, et al. (2007) Discovery of 4-aminobutyric acid derivatives possessing anticonvulsant and antinociceptive activities: a hybrid pharmacophore approach. J Med Chem 50: 2459-2467.
18. Reena TA, Seena EB, Kurup MRP (2008) Synthesis and spectral studies of cadmium (II) complexes derived from di-2-pyridyl ketone and N 4-phenylsemicarbazide: First structural report of a cadmium (II) complex of semicarbazone. Polyhedron 27: 1825-1831.
19. Casas JS, Garcia Tasende MS, Sordo J (2000) Main group metal complexes of semicarbazones and thiosemicarbazones. Coord Chem Rev 209: 197.
20. Prathapachandra Kurup MR, Varghese B, Sithambaresan M, Krishnan S, Sheeja SR, et al. (2011) Synthesis, spectral characterization and crystal structure of copper (II) complexes of 2-benzoylpyridine-N(4)-phenylsemicarbazone. Polyhedron 30: 70-78.
21. Buchholz, Nica S, Debel R, Fenn A, Breitzke H, et al. (2014) Vanadium complexes with side chain functionalized N-salicylidene hydrazides: Hydrogen-bonding relays as structural directive for supramolecular interactions. Inorg Chim Acta 420: 166-176.
22. Noblia P, Baran EJ, Otero L, Draper P, Hugo C, et al. (2004) New Vanadium(V) Complexes with Salicylaldehyde Semicarbazone Derivatives: Synthesis, Characterization, and in vitro Insulin-Mimetic Activity − Crystal Structure of [VvO2(salicylaldehyde semicarbazone)]. Eur J Inorg Chem 2004: 322-328.

23. Ivo da S Maiaa P, Deflon VM, de Sousaa GF, Lemosa SS, Batistac AA, et al. (2007) Synthesis and Characterization of Vanadium(IV) and (V) Complexes with 2-Hydroxy-acetophenone-semicarbazone (H2hasc) as Ligand. X-Ray Crystal Structures of [VO2(H2hasc)] and [VO2(Hhasc)]. Allg Chem 633: 783-789.

24. Jevtović VS, Pelosi G, Ianelli S, Kovačević RZ, Kaišarević SN (2010) Synthesis, structural studies and biological activity of a dioxovanadium (v) complex with pyridoxal semicarbazone. Acta Chim Slov 57: 363-369.

25. Djordjevic C, Puryear PC, Vuletic N, Allelt CJ, Sheffield SJ (1988) Preparation, spectroscopic properties, and characterization of novel peroxo complexes of vanadium (V) and molybdenum (VI) with nicotinic acid and nicotinic acid N-oxide. Inorg Chem 27: 2926-2932.

26. Chasteen ND, Grady JK, Holloway CF (1986) Pyrazole/imidazole and pyrazolato/imidazolato complexes of pentacyanoferrate (II/III) and pentaammineruthenium (II/III). LMCT transitions of low-spin d5 complexes. Inorg Chem 25: 2754-2763.

27. Thompson KH, McNeill JH, Orvig C (1999) Vanadium compounds as insulin mimics. Chem Rev 99: 2561-2572.

28. Thompson KH, Orvig C (2001) Coordination chemistry of vanadium in metallopharmaceutical candidate compounds. Coord Chem Rev 219: 1033-1053.

29. Rehder D (2003) Biological and medicinal aspects of vanadium. Inorg Chem Commun 6: 604-617.

30. Maurya RC, Rajput S (2007) Synthesis, Structural Characterization, and Electrochemical Studies of New Oxovanadium(V) Complexes Derived from 2-Furanoylhydrazon Derivatives. Journal of Molecular Structure 833: 133-144.

31. Lodyga-Chruscinska E, Micera G, Garribba E (2011) Complex formation in aqueous solution and in the solid state of the potent insulin-enhancing V(IV) O2+ compounds formed by picolinate and quinolinate derivatives. Inorg Chem 50: 883-899.

32. Rodrigues GDS, Da Silva Cunha I, Silva GG, De Noronha ALO, De Abreu HA, et al. (2011) DFT study of vanadyl (IV) complexes with low molecular mass ligands: Picolinate, oxalate, malonate, and maltolate. Inc Int J Quantum Chem 11: 1395-1402.

33. Jana, Konar S, Mandal TN, Kinsuk Das, Ray S, et al. (2012) Synthesis and studies of rare acylhydrazine bridged strong antiferromagnetically coupled dicopper (II) and dioxovanadium (V) complexes of a pyridyl-pyrazole derived Schiff base ligand. Polyhedron 46: 105-112.

34. Maurya MR, Bisht M, Kumar A, Kuznetsov ML, Avecilla F, et al. (2011) Synthesis, characterization, reactivity and catalytic activity of oxidovanadium (IV), oxidovanadium (V) and dioxidovanadium (V) complexes of benzimidazole modified ligands. Dalton Trans 40: 6968-6983.

35. Scior KT, Mack HG, Garcia JAG, Koch W (2008) Antidiabetic Bis-Maltolato-OxoVanadium(IV): Conversion of inactive trans- to bioactive cis-BMOV for possible binding to target PTP-1B. Drug Design Development & Therapy 2: 221-231.

36. Maurya RC, Vishwakarma PK, Mir JM, Rajak DK (2016 Oxidoperoxidomolybdenum(VI) complexes involving 4-formyl-3-methyl-1-phenyl-2-pyrazoline-5-one and some β-diketoenolates. J Therm Anal Calorim 124: 57-70 .

37. Jacob R, Fiscker GJ (2002) Mol Struct 613: 175.

38. Jayabharathi J, Thanikachalam V, Venkatesh Perumal M (2012) Characterization, photophysical and DFT calculation study on 2-(,4-difluorophenyl)-1-(4-methoxyphenyl)-1H-imidazo[4,5-f][,10] phenanthroline ligand. Spectrochim Acta A Mol Biomol Spectrosc 95: 614-621.

39. Weigel F, Hoffmann G (1976) The phosphates and arsenates of hexavalent actinides Part I Uranium. Journal of the Less Common Metals 44: 99-123.

40. Jensen BS (1959) The Synthesis of 1-Phenyl-3-methyl-4-acyl-pyrazolones-5. Acta Chem Scand 13: 1670.

41. Furman NH (1962) Standard Methods of Chemical Analysis: Industrial and natural products and noninstrumental methods I: 1211.

42. Frisch MJ, Trucks GW, Schlegel HB, Scuseria GE, Robb MA, et al. (2009) Gaussian 09. Revision A. 1. Gaussian Inc., Wallingford, CT, USA.

43. Becke AD (1993) Density-functional thermochemistry. III. The role of exact exchange. J Chem Phys 98: 5648-5652.

44. Lee C, Yang W, Parr RG (1988) Development of the Colle-Salvetti correlation-energy formula into a functional of the electron density. Phys Rev B Condens Matter 37: 785-789.

45. Saeed A, Ifzan Arshad M, Bolte M, Fantoni AC, Delgado Espinoza ZY, et al. (2016) On the roles of close shell interactions in the structure of acyl-substituted hydrazones: An experimental and theoretical approach. Spectrochim Acta A Mol Biomol Spectrosc 157: 138-145.

46. Maurya RC, Sutradhar D (2008) International J Synth Charc 1: 25.

47. Maurya RC, Rajput S (2008) International J Synth Charc 1: 101.

48. Maurya RC, Mishra DD, Pillai V (1995) Studies on some novel mixed ligand oxovanadium (1v) complexes. Synth React Inorg Met OrgChem 25: 1127.

49. Maurya RC, Patel P, Rajput S (2003) Synthesis and characterization of Mixed□Ligand Complexes of Cu (II), Ni (II), Co (II), Zn (II), Sm (III), and U (VI) O2 with a Schiff Base Derived from the Sulfa Drug Sulfamerazine and 2, 2′□Bipyridine. Synthesis and reactivity in inorganic and metal-organic chemistry 33: 801-816.

50. Garribba E, Micera G, Sanna D (2006) Inorg Chim Acta 359: 4470-4476.

51. Maurya MR, Kumar A, Abid M, Azam A (2006) Dioxovanadium (V) and μ-oxo bis [oxovanadium (V)] complexes containing thiosemicarbazone based ONS donor set and their antiamoebic activity. Inorganica chimica acta 359: 2439-2447.

52. Rayati S, Wojtczak A, Kozakiewicz A (2008) One step preparation of [(VO (μ-O) L)] 2: A 2D supramolecular network directed by intermolecular interaction. Inorganica Chimica Acta 361: 1530-1533.

53. Maurya MR, Khurana S, Zhang W, Rehder D (2002) Journal of the Chemical Society, Dalton Transactions. J Chem Soc Dalton Trans 3015.

54. Maurya MR, Khurana S, Schulzke C, Rehder D (2001) Dioxo- and Oxovanadium(V) Complexes of Biomimetic Hydrazone ONO Donor Ligands: Synthesis, Characterisation, and Reactivity. Eur J Inorg Chem 779-788.

55. Maurya RC, Mishra DD (1989) Synthesis and Characterization of Some Novel Hexa-coordinated Mixed-Ligand Cyanonitrosyl {CrNO} 5 Complexes of Chromium with some Potentially Mono- and Bi-Dentate 5-Pyrazolone Derivatives. Synth React Inorg Met Org Chem 19: 533-544.

56. Maurya MR, Kumar A, Ebel M, Rehder D (2006) Synthesis, characterization, reactivity, and catalytic potential of model vanadium (IV, V) complexes with benzimidazole-derived ONN donor ligands. Inorg Chem 45: 5924-5937.

57. Shoba D, Periandy S, Karabacak M, Ramalingam S (2011) Vibrational spectroscopy (FT-IR and FT-Raman) investigation, and hybrid computational (HF and DFT) analysis on the structure of ,3-naphthalenediol. Spectrochim Acta A Mol Biomol Spectrosc 83: 540-552.

58. Fukui K (1982) Role of frontier orbitals in chemical reactions. Science 218: 747-754.

59. Brabec CJ, Sariciftci NS, Hummelen JC (2001) Plastic Solar Cells. Adv Funct Mater 11.

60. Ebenso Eno E, Arslan T, Kandemirli F, Love I, Ogretir C, et al. (2010) Theoretical studies of some sulphonamides as corrosion inhibitors for mild steel in acidic medium. Int J Quantum Chem 110: 2614-2636.

61. Pearson RG (1993) The principle of maximum hardness. Acc Chem Res 26: 250-255.

62. Reed AE, Curtiuss LA, Weinhold F (1988) Intermolecular interactions from a natural bond orbital, donor-acceptor viewpoint. Chem Rev 88: 899-926.

63. Mulliken RS (1955) Electronic Population Analysis on LCAO–MO Molecular Wave Functions I. J Chem Phys 23: 1833.

64. Vishwakarma PK, Mir JM, Maurya RC (2016) Pyrone-based Cu(II) complexes, their characterization, DFT based conformational drift from square planar to square pyramidal geometry and biological activities. 128: 511-522